

# ANALYSIS OF THE FLUIDIZED BED DRYING OF WOOD PARTICLES

*Michael R. Milota and James B. Wilson*

Assistant Professor and Professor  
Department of Forest Products  
Oregon State University  
Corvallis, OR 97331

(Received April 1989)

## ABSTRACT

Engineering parameters necessary to design an industrial, continuous fluidized-bed dryer for wood particles were examined using a 0.21-m square batch fluidized-bed dryer. Parameters of main interest were gas velocity and drying curves, but bed voidage, particle elutriation, and distributor plate design also were considered. For unscreened (mixed sizes) hammermilled wood and sawdust, the minimum gas velocities for fluidization were 1.03 and 0.55 m/s, respectively. These values increased with increasing moisture content, decreasing sphericity, and increasing particle diameter. Current methods of adjusting batch drying curves so that they can be applied to a commercial continuous dryer were shown to be inadequate for some wood particle sizes. To predict drying curves for all particle sizes, a new method was developed that accounts for both internal and external resistances to drying. The new method was confirmed experimentally.

*Keywords:* Drying curves, moisture content, heat transfer, mass transfer, design parameters.

## INTRODUCTION

Fluidization is the process by which air passes upward through a bed of particles, suspending them in a particle-gas emulsion that behaves like a fluid—light objects float, heavy objects sink, and rising air bubbles mix the wood particles, making the emulsion appear like a boiling liquid. If the gas velocity is too low, the air percolates up through stationary particles. If it is too high, the particles are entrained as in pneumatic transport.

Widely used today for combustion and drying of granular solids in many industries, fluidization was first used in the 1920s to produce methane from powdered coal. However, the application of this technology was limited until World War II, when the increased demand for aviation fuel stimulated development of the fluidized catalytic cracking process for refining petroleum. In the forest products industry today, combustion of hogged wood fuel in boilers is the only application of fluidization, although other applications have been tested in the laboratory. Fefilov and Sokolova (1959) reported drying wood particles by fluidization, achieving water removal rates of only 130 to 220 kg hr<sup>-1</sup> m<sup>-2</sup> of bed cross section. Kobyl'skikh and Petri (1966) improved the distributor plate design and obtained water removal rates greater than 2,000 kg hr<sup>-1</sup> m<sup>-2</sup>. Kumar et al. (1971) fluidized 0.177- to 2.83-mm-diameter sawdust in a bed of sand, which enhanced heat transfer and aided fluidization. Wood particles also have been dried in suspension (Corder 1958) and in a spouting bed (Cowan et al. 1958). Paper and linerboard (Luckins and Sutherland 1962) and veneer (Carruthers and Burrige 1964; Wen and Loos 1969; Loos and Wen 1970; Loos 1971) have been dried in beds in which an inert material such as sand was fluidized and the wood material submerged into the bed to achieve a high rate of surface-heat transfer.

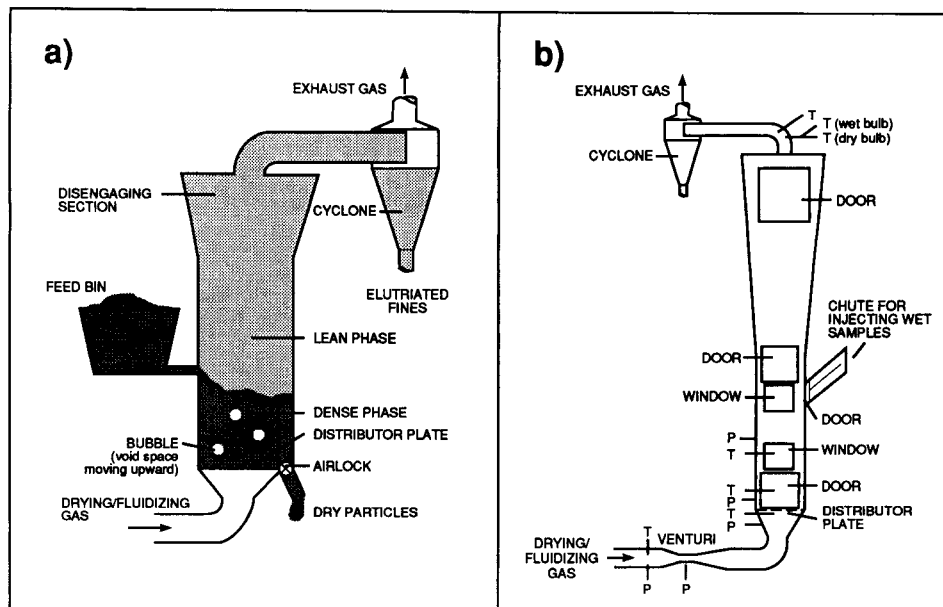


FIG. 1. a) Continuous fluidized-bed dryer which might be used industrially to dry wood particles, and b) batch fluidized-bed dryer used in this study to simulate the industrial design (T = temperature measurement, P = pressure measurement).

Fluidized beds have inherent characteristics that make them ideally suited to particle drying. The mixing action results in nearly isothermal conditions throughout the bed, good temperature control, excellent heat and mass transfer between the gas and the particles, excellent heat transfer to immersed tubes (such as those in a boiler), and ease of continuously feeding and removing particles from the bed. A uniform, well-controlled bed temperature may produce fewer hydrocarbon emissions than rotary drum dryers, which are conventionally used to dry wood particles. In addition, fluidized beds are smaller and less expensive to construct than other types of dryers of similar capacity. The disadvantages of continuous fluidized beds include nonuniform residence times and a higher air requirement than rotary dryers.

To design an industrial, continuous fluidized-bed dryer for wood particles, such as that in Fig. 1a, one must know the particles' fluidization characteristics and the drying curve of the wood material. The objective of this study was to quantify these parameters with a laboratory batch dryer so that a commercial continuous dryer can be designed. A detailed treatment of these parameters is found in Milota (1984).

#### EQUIPMENT AND MATERIALS

The laboratory batch dryer (Fig. 1b) was 2.5 m high and 0.21 m in square cross section, with windows for viewing fluidization. Wet samples were injected into the dryer through a door (60 cm above the distributor plate), which could be opened and closed while the dryer was operating. The dryer was direct-fired with natural gas.

TABLE 1. Arithmetic average of particle characteristics for screened and unscreened material dried in the batch fluidized-bed dryer.

Particle size class, by type	Screening		Hammermilled wood particles			Sawdust particles		
	Sweco mesh	Larger opening (mm)	Diameter <sup>1</sup> (mm)	Sphericity <sup>2</sup>	Voidage <sup>3</sup>	Diameter (mm)	Sphericity	Voidage
Screened								
Small	+6	—	0.68	0.60	0.49	0.80	0.64	0.45
Medium <sup>4</sup>	−6 + 12	3.35	2.03	0.51	0.54	2.18	0.68	0.53
Large	−12	1.53	3.78	0.46	0.68	4.16	0.47	0.71
Unscreened								
Mixed	—	—	1.33	0.56	0.50	1.51	0.64	0.53

<sup>1</sup> Diameter of a sphere with the same volume as the particle.

<sup>2</sup> Area of a sphere with the same volume as the particle, divided by actual particle area; equals 1 for a sphere and decreases with deviation from roundness.

<sup>3</sup> Fraction of the open area between particles; voidage presented is for beds with no airflow.

<sup>4</sup> Passes through a 3.35-mm screen but is retained by a 1.53-mm screen.

One of two 12-gauge steel distributor plates was used depending on the gas velocity: the first had 3.18-mm-diameter holes and 3.76% open area, the second 4.76-mm-diameter holes and 8.46% open area. The velocity through the holes ranged from 7 to 22 m/s, the pressure drop across the distributor plate from 3 to 10 kPa. Each plate met the design criteria in Kunii and Levenspiel (1977).

Hammermilled wood and sawdust were screened to three particle size classes (small, medium, and large). A mixed size class, consisting of 30% small, 55% medium, and 15% large particles by weight, was used to represent “unscreened” furnish whose composition could be controlled throughout the experiments. Characteristics of each size class are summarized in Table 1. Because the particles were not round, the diameters given in Table 1 are those of a sphere with the same volume as the particle. To completely express particle size, the sphericity (the area of a sphere with the same volume as the particle, divided by the actual area of the particle) also is given (Table 1). Sphericity is unity for a sphere and decreases with deviation from roundness. The packing density of the particles is described as voidage (the fraction of open area between the particles). Voidage in fluidized beds is approximately 20% greater than in beds with no airflow.

#### FLUIDIZATION CHARACTERISTICS

This study focuses on gas velocity and its effects on fluidization. Elutriation and mixing, very dependent on gas velocity, also are discussed, as are effects of particle shape. Although numerous equations exist in the literature to predict the gas velocity required to fluidize granular materials, most of these are obtained empirically using materials with much higher densities and sphericities than those of wood particles. Extrapolating these relations in an attempt to predict the minimum fluidization velocity for wood was not successful. Therefore, we undertook the following experiment.

Gas velocity was decreased in 0.05- to 0.15-m/s increments in the well-fluidized bed of the batch dryer (Fig. 1b) at room temperature until one of the following occurred: the entire emulsion was not in motion, stagnant areas were visible on the surface of the bed, channeling became excessive, or the bed surface was not level. The presence of any one of these phenomena indicated that the minimum

TABLE 2. Minimum fluidization velocities for wood particles in the batch fluidized-bed dryer. A "no" indicates no fluidization.

Moisture content (%), oven-dry basis	Velocity (m/sec), by particle size class			
	Small	Medium	Large	Mixed
Hammermilled particles, 0.15-m bed depth				
5	0.60	0.93	1.45	1.03
50	0.75	1.10	1.50	1.14
100	0.81	1.21	no	1.35
Hammermilled particles, 0.30-m bed depth				
5	0.49	1.14	no	1.08
50	0.71	1.36	no	1.26
100	no	1.43	no	1.49
Sawdust particles, 0.15-m bed depth				
5	0.26	0.54	no	0.55
50	0.48	0.86	no	0.73
100	0.91	1.05	no	1.23

fluidization velocity had been reached. Minimum fluidization velocity is an important design criterion because, at velocities lower than the minimum, the entire bed will not be well mixed, the temperature distribution may become nonuniform, and heat transfer decreases sharply.

The minimum fluidization velocities for the hammermilled wood and sawdust are given in Table 2. The velocity required for fluidization increases with particle size and moisture content because a greater pressure drop is required to support the particles as they get heavier. One of the most striking aspects of the data is that significantly greater gas velocity is required to fluidize hammermilled wood than sawdust; this difference is attributed to their respective sphericities (Table 1). The sawdust particles are less elongated, move by one another with greater ease, and are more readily fluidized than the hammermilled particles.

In the cases in which the large particles would not fluidize, either a large channel formed in the center of the bed or the particles interlocked and "bridged" across the bed. A larger bed-to-particle size ratio would probably help eliminate both of these phenomena. In the one case in which small particles would not fluidize, the high moisture content caused particle agglomeration and channeling. Achieving fluidization above 100% moisture content was unpredictable.

Under all test conditions, the mixed particles were well fluidized at a velocity 1.2 to 1.5 times the minimum. This is important in an industrial situation because it suggests that material would not have to be screened for fluidization. Poor fluidization at high moisture contents is not a problem either because wet material entering a continuous dryer immediately mixes with the dry material already in the bed. The mixing of wet and dry material results in an average bed moisture content which can be controlled.

Practically speaking, gas velocity reaches maximum when an unacceptable amount of material is elutriated. The amount of elutriated fines was a small fraction of the total bed weight, only 0.8 to 9.4% after 34 minutes of bed operation, and could be mixed with the main exit stream from the dryer.

For a low-density material such as wood, special attention should be paid to

distributor plate design. If the open area is too small, gas velocity through the holes in the plate will be too high. Because the resulting kinetic energy of the jet of gas is greater than the resistance of the bed, the gas punches up through the bed, failing to contact the particles.

## DRYING CURVES

### *Background*

The drying curve,  $M(t)$ , is the relationship between the moisture content ( $M$ ) of a particle and the length of time ( $t$ ) it has been in the dryer. Establishing the drying curve using a continuous fluidized-bed dryer is impractical; therefore, Vanecek et al. (1962) proposed a method using batch drying, in which a small amount of wet material is placed in a large amount of dry material to simulate continuous drying. This method has been shown to be reliable, but controlling the inlet temperature well enough to maintain a constant bed temperature is difficult.

Reay and Allen (1982a) solved the problem of inlet temperature control by using a constant inlet temperature (isothermal inlet, *ii*), allowing the bed temperature to vary, and proposing a transformation to convert the drying conditions in the bed to constant temperature (isothermal bed, *ib*). To make the transformation, the experimental isothermal-inlet curve is divided into equal time intervals,  $(\Delta t)_{ii}$  (Fig. 2). For each interval, the actual conditions in the dryer are compared to the new isothermal-bed conditions;  $(\Delta t)_{ii}$  is lengthened if the new conditions are less severe than the actual conditions or shortened if the new conditions are more severe. Conditions are considered more severe if the gas temperature or velocity is higher or the equilibrium moisture content or bed weight lower. For example, in Fig. 2, because the new condition is less severe, the first interval (the time to reach 60% moisture content) was lengthened. The cumulative time of these new intervals,  $(\Delta t)_{ib}$ , determines the position of the new drying curve. In practice, the original intervals are as short as is practical.

How much to shorten or lengthen a time interval is determined with ratios. Differences in bed temperature are accounted for with two ratios: the ratio of the difference between the saturated vapor pressure,  $p_v^s$ , and the partial pressure of water vapor at the dryer inlet,  $p_v^i$ , for each condition, and the ratio of the difference between the current moisture content,  $M$ , and the equilibrium moisture content,  $M_{eq}$ , for each condition. For all materials, bed temperature is corrected with Eq. (1):

$$(\Delta t)'_{ib} = (\Delta t)_{ii} \left[ \frac{[(p_v^s - p_v^i)(M - M_{eq})]_{ii}}{[(p_v^s - p_v^i)(M - M_{eq})]_{ib}} \right] \quad (1)$$

For materials in which drying is controlled by factors internal to the particle, no further transformations are used. For other materials, the gas velocity,  $u_o$ , and bed weight,  $w$ , must be considered, again with ratios, one interval at a time, as in Eq. (2):

$$(\Delta t)_{ib} = (\Delta t)'_{ib} \left[ \frac{(u_o)_{ii}(w)_{ib}}{(u_o)_{ib}(w)_{ii}} \right] \quad (2)$$

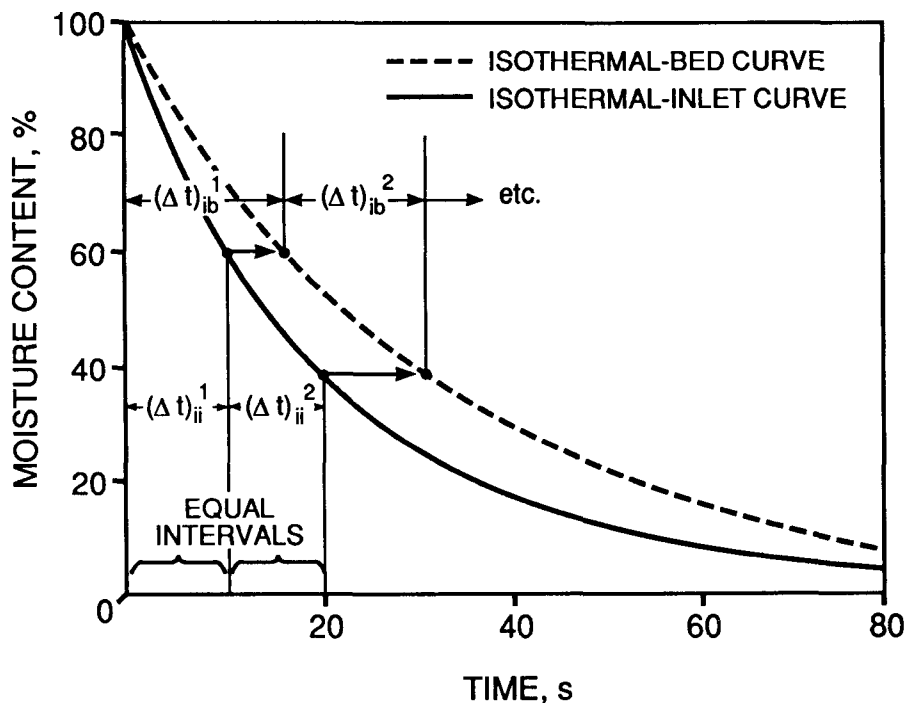


FIG. 2. Converting the isothermal-inlet dryer curve to the isothermal-bed drying curve. Superscripts 1 and 2 denote the first and second time intervals, respectively.

Generally, Eqs. (1) and (2) provide a way to predict drying curves for new bed conditions from drying curves for known bed conditions. However, these equations have limited applicability to drying curves for wood particles in fluidized beds, as will be shown.

#### *Current study*

Drying curves were determined following the method of Vanecek et al. (1962). To do this, 1.5 kg of dry, mixed wood particles were fluidized in the batch dryer (Fig. 1b) and steady-state conditions obtained. A 0.25-kg sample of wet particles from one of the four size classes (small, medium, large, mixed) was then injected into the dryer. Bed temperature and exit gas humidity were monitored while the sample dried from an initial moisture content ranging from 100 to 120% (oven-dry basis) to an equilibrium moisture content of approximately 0%. Drying times ranged from 1 to 3 minutes. The exit gas humidity was used for performing a mass balance on the inlet and outlet gas; from this, the moisture content of the particles as a function of time was calculated and the drying curve plotted. If the mass balance on water vapor differed from the weight change of the particles by more than 10%, the run was repeated. Fines collected from the cyclone had a moisture content of 2 to 4%.

Following this procedure, isothermal-inlet drying curves were generated for inlet temperatures of 127, 167, and 207 C and gas velocities of 1.6 and 2 m/s. Six of these curves are shown for small, hammermilled wood particles (Fig. 3a).

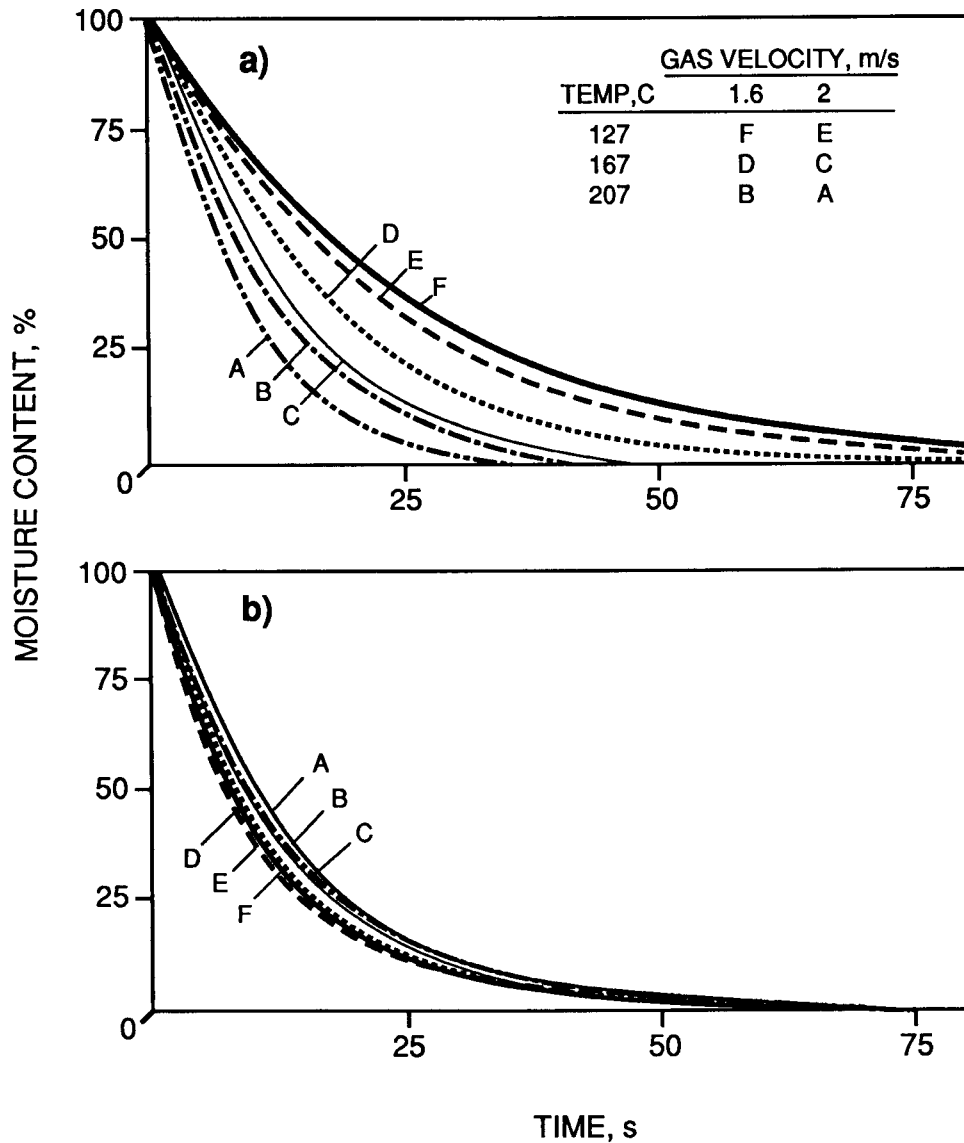


FIG. 3. a) Isothermal-inlet drying curves for small, hammermilled wood particles under various test conditions, transformed to b) isothermal-bed drying curves at 80 C and 1.5 m/s by text Eqs. (1) and (2).

These experimental curves were then transformed with Eqs. (1) and (2) to isothermal-bed drying curves for a new temperature (80 C) and gas velocity (1.5 m/s) (Fig. 3b). The six curves in Fig. 3a, produced independently at six different conditions, predicted highly similar isothermal-bed drying curves, indicating that Eqs. (1) and (2) are valid for small wood particles.

However, when the same technique was applied to large particles, the isothermal-inlet curves did not predict similar isothermal-bed curves. Nor did using

only Eq. (1) improve the grouping of the lines. This outcome suggests that the method may not be satisfactory for large wood particles and that a different transform equation was needed to account for both internal and external factors controlling the drying rate of large wood particles. The technique was more satisfactory for medium than large wood particles, although not as effective as for small wood particles.

The new transform equation uses the Biot number (Bi), a ratio of the internal and external resistances to heat transfer, to generate valid drying curves for a range of particle sizes. For example,  $Bi = 3$  indicates that the total resistance is 75% due to internal factors and 25% due to external factors. In the work of Reay and Allen (1982b), the resistance was very clearly external in the cases of iron ore and ion exchange resin ( $Bi < 0.1$ ) and very clearly internal in the case of wheat ( $Bi > 20$ ). The subsequent discussion centers on how to apportion these effects so that the internal and external factors are properly accounted for in the analysis.

Of the internal factors, vapor diffusion is assumed to be the main path for moisture movement. Rate of vapor diffusion is proportional to absolute temperature,  $T$ , to the 1.75 power (Kanury 1975) such that

$$R_i = \left[ \frac{(T + 273)_{ii}}{(T + 273)_{ib}} \right]^{1.75} \quad (3)$$

where  $R_i$  is the resistance ratio between bed conditions due to internal factors. Of the external factors, the ratio of the pressure terms,  $p_v^s$  and  $p_v^i$ , accounts for bed temperature and velocity is accounted for as in Eq. (2) such that

$$R_e = \left[ \frac{(p_v^s - p_v^i)_{ii}}{(p_v^s - p_v^i)_{ib}} \right] \left[ \frac{(u_0)_{ii}}{(u_0)_{ib}} \right] \quad (4)$$

where  $R_e$  is the resistance ratio between bed conditions due to external factors.

The Biot number and the internal and external resistance ratios were then combined to form the new transform equation:

$$(\Delta t)_{ib} = (\Delta t)_{ii} \left\{ \left( \frac{1}{Bi + 1} \right) R_e + \left[ 1 - \left( \frac{1}{Bi + 1} \right) \right] R_i \right\} \quad (5)$$

where  $1/(Bi + 1)$  is the fraction of the total resistance external to the particle.

Equation (5) is applied like Eqs. (1) and (2) (see Fig. 2). In this study, the experimental isothermal-inlet drying curves for all sizes of hammermilled wood and sawdust were successfully transformed with Eq. (5). Examples of the new predicted isothermal-bed drying curves are shown in Figs. 4a and b, respectively. In each case, the six independently produced isothermal-inlet curves predicted highly similar isothermal-bed drying curves at the selected condition (80 C, 1.5 m/s). In the case of the small particles, the curve predicted by Eqs. (1) and (2) in Fig. 3a and the new curve predicted by Eq. (5) in Fig. 4a are essentially the same. This is expected for the small particles because Bi is small (range, 0.2 to 0.5) and internal resistance minimal. In the case of the large particles, Bi is much larger



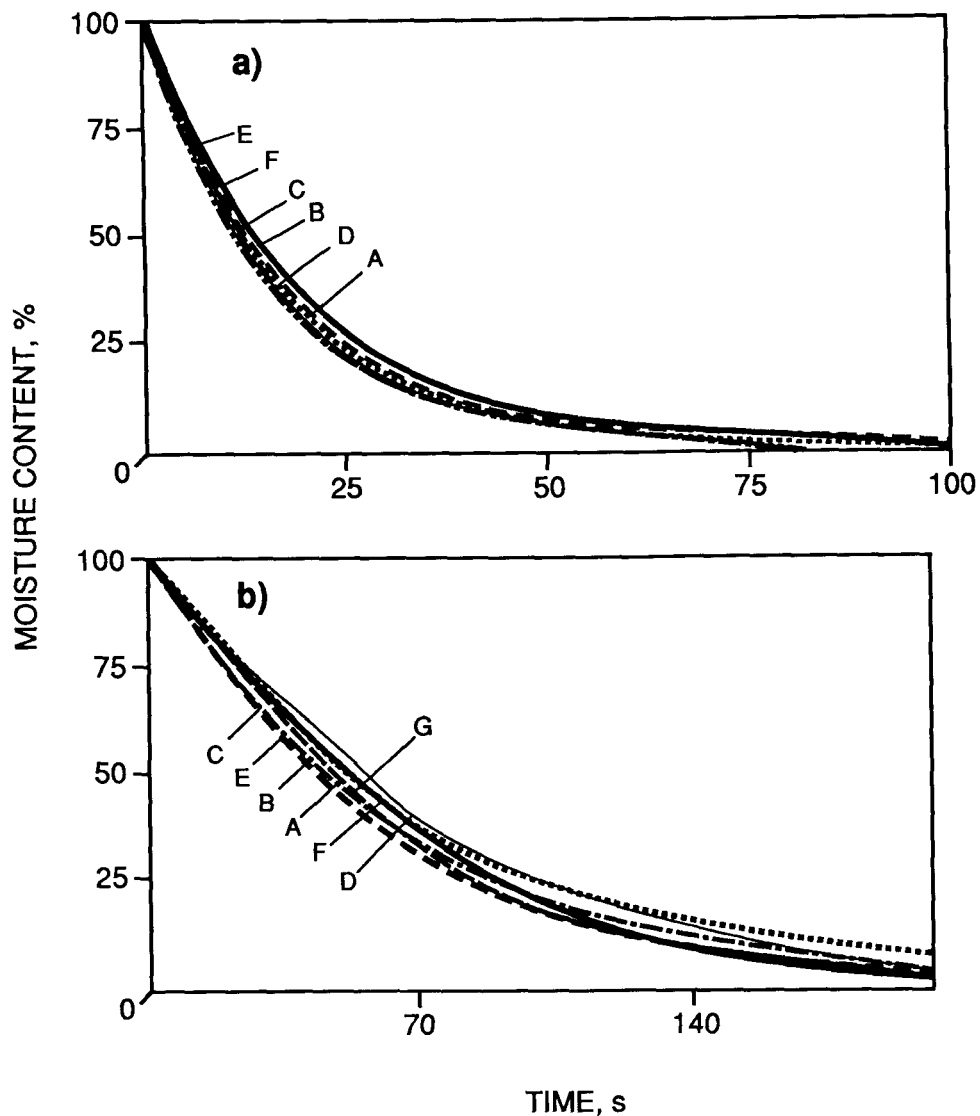


FIG. 4. Isothermal-bed drying curves at 80 C and 1.5 m/s for a) small and b) large hammermilled wood particles. Curves in both a) and b) were converted with the new transform equation, Eq. (5). Those in a) were converted from the isothermal-inlet curves in Fig. 3a. Those in b) were converted from the isothermal-inlet curves for large particles (not shown); those curves were generated under the same six conditions as for the small particles in Fig. 3a. Curve G in b) experimentally verified the predicted curves.

(range, 1 to 5) and internal resistance significant. However, the new transform equation properly accounts for these factors, yielding the excellent agreement of the curves shown in Fig. 4b.

The position of the predicted drying curves for large particles (Fig. 4b) was experimentally verified by manually maintaining the isothermal-bed temperature.

Otherwise, sample size and procedures were similar to those of the isothermal-inlet experiments. Maintaining a constant bed temperature is difficult because temperature fluctuates rapidly early in the run. However, the result, curve G in Fig. 4b, agrees well with the predicted curves, thus validating the analytical procedure.

#### CONCLUSIONS

Wood behaves differently than other commonly fluidized materials because it has lower density, higher voidage, lower sphericity, and generally a larger range of particle sizes. Even when the unscreened (mixed sizes) sawdust and hammermilled wood were compared, the minimum fluidization velocity differed by a factor of two. Therefore, bench-scale testing is necessary to determine the minimum fluidization velocity for each furnish before industrial design so the dryer will operate properly.

Below the gas velocities that adequately fluidized unscreened hammermilled particles (range, 1.2 to 2.5 m/s) and sawdust (range, 0.7 to 2 m/s), small temporary channels develop; at higher velocities, elutriation becomes significant. In the batch dryer, very wet (>100% moisture content) material tends to agglomerate and promote channeling. In a continuous dryer, however, the average bed moisture content would be low enough that this would not be a problem.

Drying curves for wood particles can be established by batch drying a small amount of wet material in a large amount of dry material while a gas inlet temperature is held constant. Designers of continuous dryers can use the method developed in this paper to transform the experimental drying curve to an isothermal-bed drying curve for wood particles. This method, similar to that of Reay and Allen (1982a, b), better accounts for the heat and mass transfer characteristics of wood particles. The resulting isothermal-bed drying curves agree well with experimental data.

#### ACKNOWLEDGMENTS

This is paper 2256, Forest Research Laboratory, Oregon State University, Corvallis.

#### REFERENCES

- CARRUTHERS, J. F. S., AND M. S. BURRIDGE. 1964. The drying of veneers in a fluid bed. *For. Prod. J.* 14(6):251-253.
- CORDER, S. E. 1958. Suspension drying of sawdust. *For. Prod. J.* 8(1):5-10.
- COWAN, C. B., W. S. PETERSON, AND G. L. OSBERG. 1958. Spouting of large particles. *Eng. J.* 41(5):60-64.
- FEFILOV, V. V., AND A. I. SOKOLOVA. 1959. Drying of wood particles in a fluidized bed. *Sb. Tr. Tsentr. Nauchno-Issled. Lesokhim. Inst.* 13:3-15.
- KANURY, A. M. 1975. *Introduction to combustion phenomena.* Gordon and Breach, New York.
- KOBYL'SKIKH, A. P., AND V. N. PETRI. 1966. Drying sawdust in a fluidized bed. *Derevoobrab. Promst.* 15(7):7.
- KUMAR, R., K. V. BALACHANDRAN, AND R. N. KUMAR. 1971. Preliminary studies on the drying of sawdust in a fluidized bed. *J. Indian Acad. Wood Sci.* 2(1):32-37.
- KUNII, D., AND O. LEVENSPIEL. 1977. *Fluidization engineering.* John Krieger Publishing, Inc., New York.
- LOOS, W. E. 1971. Fluidized bed drying of southern pine veneer. *For. Prod. J.* 21(12):44-49.
- , AND C. Y. WEN. 1970. Fluidized bed drying of yellow poplar veneer. *For. Prod. J.* 20(6):56-58.

- LUCKINS, J., AND C. A. O. SUTHERLAND. 1962. Fluidized bed drying of paper and board. Pages 238–242 *in* Proceedings from the Symposium on the Interactions between Fluids and Particles, London. Institute of Chemical Engineering, New York.
- MILOTA, M. R. 1984. Engineering study on the drying wood particles in a fluidized bed. Ph.D. dissertation, Oregon State University, Corvallis.
- REAY, D., AND R. W. K. ALLEN. 1982a. The effect of temperature on fluid bed batch drying curves. *J. Sep. Process Technol.* 3(4):11–13.
- , AND ———. 1982b. Predicting the performance of a continuous, well-mixed fluidized bed dryer from batch tests. Pages 130–140 *in* Proceedings of the Third International Drying Symposium. Hemisphere, New York.
- VANECEK, V., R. DRBOHLAV, AND M. MARKVART. 1962. Calculation of continuous fluidized bed drying equipment based on laboratory tests. Pages 233–237 *in* Symposium on the Interaction between Fluids and Particles, London. Institute of Chemical Engineering, New York.
- WEN, C. Y., AND W. E. LOOS. 1969. Rate of veneer drying in a fluidized bed. *Wood Sci.* 2(2): 87–90.